



Universiteit  
Leiden  
The Netherlands

## Metabolomics study of blood vessels-on-chip model

Kallakkudi Pandian, K.

### Citation

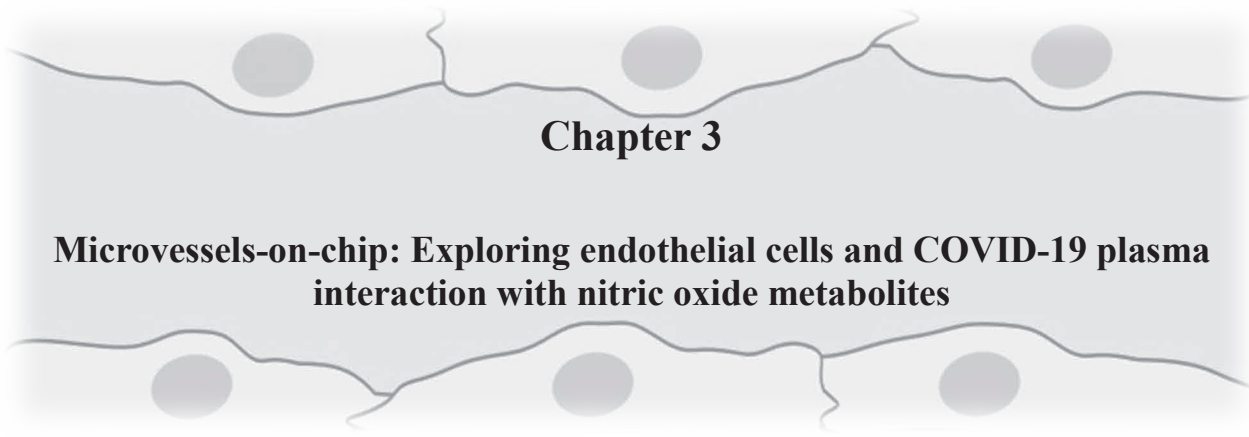
Kallakkudi Pandian, K. (2025, March 26). *Metabolomics study of blood vessels-on-chip model*. Retrieved from <https://hdl.handle.net/1887/4209144>

Version: Publisher's Version

License: [Licence agreement concerning inclusion of doctoral thesis in the Institutional Repository of the University of Leiden](#)

Downloaded from: <https://hdl.handle.net/1887/4209144>

**Note:** To cite this publication please use the final published version (if applicable).



**Chapter 3**

**Microvessels-on-chip: Exploring endothelial cells and COVID-19 plasma interaction with nitric oxide metabolites**

**Kanchana Pandian, Rudmer Postma, Anton Jan van Zonneveld, Amy Harms\* and  
Thomas Hankemeier\***

\*These authors are co-corresponding authors

*Nitric Oxide*. 155, 12-19. Doi: [org/10.1016/j.niox.2025.01.002](https://doi.org/10.1016/j.niox.2025.01.002)

### Abstract

COVID-19, caused by the severe acute respiratory syndrome coronavirus 2 (SARS-CoV-2), primarily manifests as a flu-like illness with lung injury, often necessitating supplemental oxygen. Elderly individuals and those with pre-existing cardiovascular diseases are at increased risk of mortality. The endothelial barrier disruption observed in patients indicates systemic viral invasion and widespread endotheliitis. Endothelial dysfunction, characterized by impaired nitric oxide (NO) production, contributes to vasoconstriction, inflammation, and coagulation abnormalities seen in COVID-19. In this study, we investigated the impact of COVID-19 patient-derived plasma on the endothelium through NO metabolite analysis using an *in vitro* 3D micro vessel model. Our experiments revealed alterations in NO metabolites in response to COVID-19 patient plasma perfusion, with BH<sub>4</sub>+BH<sub>2</sub> supplementation improving citrulline levels in severe COVID-19 patient models. Positive correlation between arginase activity and eNOS activity was observed in the severe COVID-19 patient model but not in the mild COVID-19 patient model. These findings underscore the importance of endothelial dysfunction in COVID-19 pathogenesis and highlight potential therapeutic targets for mitigating vascular complications associated with severe infection.

### ***Key words***

Endothelial dysfunction, COVID-19, Nitric Oxide, Biopterin, Endothelial Nitric Oxide Synthase, Arginase, 3D microvessels-on-chip model

## **Introduction**

COVID-19, an illness resulting from infection with the severe acute respiratory syndrome coronavirus 2 (SARS-CoV-2), manifests as a respiratory infection, with 24% to 54% of severe cases exhibiting lung injury, often requiring supplemental oxygen [1]. Individuals aged 60 and above, especially those with pre-existing cardiovascular diseases, experience higher mortality rates.

Patients with rapid clinical deterioration and multi-organ failure often show evidence of systemic endotheliitis [2,3], indicating a break in the endothelial barrier that allows systemic viral invasion. In particular, the impaired vascular homeostasis secondary to the structural and functional damage of the endothelium and its main component, the endothelial cells, contributes to the systemic proinflammatory state and the multiorgan involvement observed in COVID-19 patients. [4]. In previous studies, COVID-19 was related to endothelial dysfunction, due to direct (endothelial cells are infected by the virus) and indirect damage (systemic inflammation) factors [5,6]. Vasoconstrictive, proinflammatory, and pro-coagulant states, along with subsequent organ ischemia and tissue edema, result from endothelial dysfunction observed in COVID-19, possibly resulting from direct viral infection or an excessive inflammatory response triggered by neighboring epithelial cell infection and high levels of pro-inflammatory cytokines [7].

A characteristic feature of endothelial dysfunction is the inhibition of endothelial nitric oxide synthase (eNOS), leading to a concurrent deficiency in nitric oxide (NO) production [8], explaining the elevated risk of adverse outcomes in COVID-19 for individuals with pre-existing endothelial dysfunction. The human aging process leads to vascular endothelial dysfunction, characterized by an imbalance between vasodilators and vasoconstrictors produced by the endothelium [9] and lower NO production in the elderly, likely making them more susceptible for COVID-19 related complications [10,11]. Akaberi et al. established a correlation between NO levels and COVID severity, demonstrating that NO derived from S-nitroso-N-acetyl penicillamine (SNAP) can effectively delay or entirely prevent the development of the SARS-CoV-2 viral cytopathic effect in treated cells and inhibit viral replication [12]. Inhaled NO gas has emerged as a

potential therapeutic process to enhance patient oxygenation and potentially improve clinical outcomes [13]. However, the complications associated with direct NO inhalation result in the conversion of NO to nitrogen dioxide, a toxic gas with no therapeutic value [14]. Potential therapeutic mechanisms encompass vasodilation by improving the NO levels, antiviral, anti-inflammatory, and antithrombotic properties.

Healthy ECs utilize L-arginine as a substrate for endothelial nitric oxide synthase (eNOS) to produce NO and L-citrulline, in conjugation with NADPH, molecular oxygen, and tetrahydrobiopterin (BH4) [15]. Endothelial dysfunction can be caused by several factors, including inflammation, hypoxia, metabolic and behavioral factors, as well as mechanical issues such as reduced blood flow. These factors contribute to decreased production of nitric oxide (NO) due to the inadequate availability of the substrate (L-arginine) and cofactor (BH4), resulting in the uncoupling of endothelial nitric oxide synthase (eNOS) from its substrate—a phenomenon also observed in COVID-19. A previous study by Gomez et al., showed that increase in arginine levels and decrease in citrulline levels may be indicative of a deficiency in the cofactor, leading to eNOS uncoupling from arginine and consequently reduced conversion to citrulline or NO [16]. Infusion of BH4 in coronary artery disease patients showed improved effect of vasodilation [17] and adding dietary sources of nitrates and nitrites containing food to the regular diet improves immunity and NO was considered as a potential targeted therapy by improving NO production [18]. However, there have been no studies conducted in COVID-19 patients demonstrating that BH4 supplementation improves vasodilation or reverses endothelial dysfunction. It is important to consider that enhancing NO production is viewed as one of the key treatment strategies due to its antiviral and anti-inflammatory properties [19]. Microvascular complications and endothelial dysfunction are frequently seen in deceased COVID-19 patients.

The precise role of endothelial dysfunction, whether triggered by inflammation or caused by SARS-CoV-2 pathogenesis, in disrupting nitric oxide metabolism remains a topic of active investigation. A key limitation of current in vitro models of COVID-19 is the incomplete understanding of how specific components within COVID-19 patient plasma impact the eNOS pathway, particularly the conversion of arginine to citrulline and

ornithine. A critical gap exists in translating previous work on models for endothelial dysfunction to the specific context of COVID-19. A study utilizing a 3D endothelial model on a microfluidic chip has provided insights into Ebola virus-hemorrhagic fever syndrome [20] and another study employed an effective 3D microvascular model to investigate the influence of blood plasma components on microvascular integrity [21].

Given the importance of 3D model architecture, our study focusses on the impact of COVID-19 plasma components using a 3D endothelial system through the analysis of metabolites involved in the production of NO. We conducted *in vitro* perfusion experiments using an endothelial 3D microvessels cell model developed in our previous work [22] to study the impact of COVID-19 patient-derived plasma from severe and mild cases, enriched with  $^{13}\text{C}_6, ^{15}\text{N}_4$  L-arginine (arginine+10), on endothelial cells. Our 3D microvessels model utilizes MIMETAS rerouted 2-lane OrganoPlate which incorporates collagen as the extracellular matrix, with a specifically designed tubular channel mimicking a microvessels lumen. We conducted an observational pilot-case study using two COVID-19 patient's blood samples. Following sample collection, analysis was conducted to identify downstream metabolites indicative of NO production. The eNOS enzyme activity was assessed by measuring the conversion of the NO substrate, arginine+10, to  $^{13}\text{C}_6, ^{15}\text{N}_3$  L-Citrulline (citrulline+9). Additionally, we examined the generation of  $^{13}\text{C}_5, ^{15}\text{N}_2$  L-Ornithine (ornithine+7) by the arginase enzyme, which also utilizes L-arginine as a substrate. We supplemented the perfused plasma within the microvessels with the eNOS enzyme stimulator VEGF, the inhibitor L-NAME, and the arginase enzyme inhibitor BEC. Significantly, we observed the impact of BH4+BH2 in the interaction between COVID-19 plasma and endothelial cells by monitoring changes in citrulline levels after supplementing the plasma with the cofactor BH4+BH2. The obtained results confirm that supplementation of BH4+BH2 could improve the citrulline level in severe COVID-19 patients. Furthermore, the significant correlation observed between arginase activity and eNOS activity after BH4+BH2 supplementation in COVID patients suggests a potential diagnostic marker, whereby enhanced citrulline levels and reduced ornithine levels could be indicative of healthy status.

## Material and Methods

### *Patient study*

We conducted an observational case pilot study of two patients with a diagnosis of COVID-19, whose blood samples were collected at the time they were admitted to the intensive care unit with a COVID-19 diagnosis. Enrolled subjects were classified as severe (with high viral load) or mild (minimal viral load) COVID-19 with their clinical blood reports shown in **Table. 1**. Plasma from healthy individuals (Female 20-30 years old) were used as controls for each COVID-19 patient. The approximate range of CRP level in age-based COVID-19 patient's CRP levels were evaluated in earlier studies [23]. According to that, elevated CRP levels correlate with the severity of COVID-19. In our study, the severely ill COVID-19 patient (a 65-year-old female) who was deceased exhibited significantly higher CRP levels compared to the mildly ill COVID-19 patient (a 45-year-old female) who survived. The use of human samples in this study was approved by the METC Leiden-Den-Haag. The study code was P20.051 and the CCMO code was NL73762.058.20. Informed consent was obtained from all participants. All experiments were conducted in accordance with ethical guidelines and relevant regulations.

Patient details & clinical report	COVID-19 - severe (patient 1 - PT1)	COVID-19 – mild (patient 2 - PT2)	Healthy control - Normal range	References
Gender and age	Female - 65	Female - 45		
Creatinine (µMol/L)	152	66	44 - 97	[24]
Urea (mMol/L)	9.2	2.3	1.8 to 7.1	[24]
Albumin (g/L)	32	41	34 - 54	[25]
Estimated glomerular filtration rate (EGFR) (mL/min)	31	90	90 - 120	[26]
Viral load in throat (copies/ml)	59630	887		
CRP (mg/L)	66.9	3.0	Less than 10.0	[27]

**Table 1.** Clinical characteristics of severely (PT1) and mildly (PT2) infected COVID-19 patients. CRP – C-reactive protein. Highlighted in red indicates deviation from the normal range.

### *Cell culture*

Human coronary artery endothelial cells (HCAECs) (PromoCell, Netherlands) were resuspended in 10 ml fresh EGM MV2 medium with supplements (PromoCell, Netherlands) and cultured in T75 flasks (Nunc Easyflask, Sigma, Netherlands). Cell cultures were maintained at 37°C with 5% CO<sub>2</sub> and media was refreshed three times a week. Cells were detached at 85% confluence with 0.25 % Trypsin EDTA (Lonza, Netherlands) and cell pellets were collected by centrifugation at 300g for 5 minutes.

For the microvessel model, HCAECs were seeded in the re-routed OrganoPlate (MIMETAS, Netherlands), following the protocol described in the referenced work [22]. The microvessels-on-chip model is shown in the **Supplementary Fig. 1**. Once the cells were confluent, media in microvessels were replaced with fresh EGM MV2 media and the OrganoPlate was attached to the microfluidic pump with set 5 dyne/cm<sup>2</sup> shear stress using LabView software. The setup was kept in the incubator and the flow of media through the chips was maintained for 6 hours with unidirectional flow followed by perfusion of plasma through the microvessels is described in next section.

### *Plasma assay and perfusing human blood plasma in microvessels in vitro*

The collected EDTA blood samples were centrifuged to isolate the plasma fractions (2 x 15 minutes at 2500 g) and stored in -80°C for further experiments.

EDTA plasma samples were initially treated with 1 μM hirudin (94581 – 1EA, Sigma-Aldrich), 50 μg/ml CTI (CTI -01, Haematologic Technologies), and 25 μM compstatin. Subsequently, the samples were recalcified with 3.1 mM CaCl<sub>2</sub>. These treated samples were then combined with 50% SILAC media containing 150μM of <sup>13</sup>C<sub>6</sub>, <sup>15</sup>N<sub>4</sub>-L-

arginine. After 6 hours of unidirectional flow with the cell growth media (EGM MV2), microvessels were exposed to the cocktail mix of either healthy or COVID-19 plasma supplemented with 150 $\mu$ M of  $^{13}\text{C}_6$ ,  $^{15}\text{N}_4$ -L-arginine (CORTECNET, Netherlands) and different stimulatory and inhibitory compounds and cofactor BH4+BH2. The oxidation of the BH4 was seen leading to BH2, therefore we represented cofactor treatment as BH4+BH2 to indicate the presence of both BH4 and BH2. This treatment was conducted at 37°C with 5% CO<sub>2</sub> for 12 hours by placing the OrganoPlate on the rocker platform that generates bidirectional fluid flow. The experimental conditions are listed below in **Table. 2**.

Compound exposure and conditions	Concentrations
Blank	Working solution
Control	Working solution perfused into the microvessels
BH4+BH2	10 $\mu$ M
VEGF	20ng/ml, 50ng/ml and 100ng/ml
L-NAME	1 mM
VEGF + L-NAME	100ng/ml + 1mM
VEGF + BEC	100ng/ml + 100 $\mu$ M
L-NAME + BEC	1mM + 100 $\mu$ M
iArg (isotope labeled arginine)	500 $\mu$ M

**Table 2.** Experimental conditions and concentrations of stimulatory and inhibitory compounds of eNOS and arginase enzyme was prepared in working solution. Note: Working solution composition - Healthy or COVID-19 plasma (50%) + 150 $\mu$ M of  $^{13}\text{C}_6$ ,  $^{15}\text{N}_4$ -L-arginine in 50% SILAC media.

iArg composition, 50% of healthy or COVID plasma (50%) + 500  $\mu\text{M}$  of  $^{13}\text{C}_6$ ,  $^{15}\text{N}_4$ -L-arginine in 50% SILAC media.

Following the application of shear stress and compound treatments, samples were collected, from the outlet of each microvessels, snap frozen with liquid nitrogen and stored at  $-80^\circ\text{C}$  for LCMS analysis.

### ***Metabolic profiling using ultra-high performance liquid chromatography - mass spectrometry (UPLC- MS/MS)***

Samples were analyzed using a method based on previous work [22] using an amine profiling platform that employed an AccQ-Tag derivatization strategy, adapted from the protocol provided by Waters [28]. The microvessels-treated plasma samples (10  $\mu\text{L}$ ) were thawed on ice. Quality control (QC) samples were generated by pooling equal volumes of all media + plasma samples, and 10  $\mu\text{L}$  of this pool underwent the same process as individual samples. For reduction and deproteination, water (5  $\mu\text{L}$ ), Tris-(2-carboxyethyl) phosphine hydrochloride (TCEP) (10  $\mu\text{L}$ ), and absolute methanol (75  $\mu\text{L}$ ) were added. After centrifugation at 12000g for 10 minutes, the supernatant was transferred to a fresh Eppendorf tube and dried under vacuum. The dried residue was reconstituted in borate buffer – pH 9 (10  $\mu\text{L}$ ) vortexed for 10s and treated with 2.5  $\mu\text{L}$  of AccQ-TagAQC derivatization reagent (Waters, Waters B.V. Art. No. 186003836, The Netherlands). The samples were then kept at  $55^\circ\text{C}$  for 30 minutes in a shaker (Incubating microplate shaker, VWR, The Netherlands), 20% of formic acid (5  $\mu\text{L}$ ) was added for neutralization. After a quick vortex, each sample was transferred to the autosampler vial for LC-MS injection.

Three  $\mu\text{L}$  of sample solution was injected onto a UPLC Class I (Acquity, Waters Chromatography Europe BV, Etten-Leur, The Netherlands) system with an AccQ-Tag Ultra C18 Column (1.7  $\mu\text{m}$ , 100 x 2.1 mm, Waters, Ireland) coupled to a Sciex QTRAP® 6500 mass spectrometer [28]. Liquid chromatography (LC) separation and mass spectrometry parameters were the same from the work [22].

The compound list with target  $m/z$  for precursor and product ions is shown in Supplementary Table 1. Raw LC-MS/MS data was processed with AB Sciex PeakView™

2.0 and MultiQuant™ 3.0.1 software for targeted metabolite peak identification and integration.

### *Statistical analysis*

Box plots were created with GraphPad Prism 9.3.1 software. Significance is determined by a two-way ANOVA- multiple comparison test and student's t-test. In this study, correlation analysis was performed between the three treatment groups (healthy, mild COVID-19, and severe COVID-19) using a Pearson Correlation coefficient with a significance threshold of  $p > 0.05$ . All biological and technical replicates were included in the analysis.

## **Results**

This study utilized a microfluidic chip model to investigate how COVID-19 infection affects eNOS-derived nitric oxide metabolite production. We cultured microvessels in the rerouted OrganoPlate using HCAECs and exposed them to plasma from COVID-19 patients (mild and severe) and healthy controls. By measuring metabolites like citrulline+9 and ornithine+7, we compared metabolite levels across groups to understand the impact of COVID-19.

### *Measurement of nitric oxide metabolites from severe COVID-19 patient plasma perfused 3D microvessels.*

Differences in NO metabolites assessed using UPLC-MS/MS in a severely infected COVID-19 patient compared with a healthy control are shown in **Fig. 1 A-C**. Before the cells were exposed to the plasma samples, the direct measurement of plasma levels of unlabeled arginine, citrulline, and ornithine showed no difference between healthy and COVID-19 (**Supplementary Fig. 2 A-C**).

In the context of COVID-19, the addition of the eNOS stimulator VEGF at varying concentrations in the presence of BH<sub>4</sub>+BH<sub>2</sub> resulted in an elevated ratio of L-citrulline+<sup>9</sup>/L-arginine+<sup>10</sup>. However, when BH<sub>4</sub>+BH<sub>2</sub> was not added to VEGF (50ng), no significant difference was observed. Arginase inhibition using BEC treatments resulted in only slightly elevated levels of citrulline+<sup>9</sup>/arginine+<sup>10</sup> ratio in both healthy and COVID-19 models (**Fig. 1A**). The ratio of citrulline+<sup>9</sup>/ornithine+<sup>7</sup> (**Fig. 1B**) showed no significant difference in any of the conditions in COVID-19, compared to the healthy plasma control, suggesting that there are no changes in the relative activity of eNOS to arginase. However, when evaluating the ratio of ornithine+<sup>7</sup>/arginine+<sup>10</sup> (**Fig. 1C**), the arginase inhibition by BEC showed reduced levels with a non-significant difference and a higher ratio was observed in VEGF (100ng) in the presence of BH<sub>4</sub>+BH<sub>2</sub>. This suggests that at higher concentration of VEGF, the utilization of arginine by arginase in COVID conditions was significantly higher.

Numerous research efforts have delved into enhancing NO production by administering higher L-arginine concentrations to address substrate deficiency in endothelial dysfunction, our study did not reveal any significant difference between healthy and COVID-19. To understand the impact of COVID on substrate availability, arginine bioavailability was assessed but no significant difference was seen between healthy and COVID-19 conditions (result not shown). Correlation analysis was conducted to assess the relationship between eNOS and arginase enzyme activity. In the healthy cohort (**Fig. 1D**), the correlation analysis revealed an association between eNOS and arginase enzyme activity ( $r = -0.01$ ,  $p$  value = 0.9) and in severe COVID-19 patient, the correlation analysis revealed a significant association between eNOS and arginase enzyme activity ( $r = 0.3$ ,  $P = 0.02$ ), indicating a positive relationship between the two variables. (**Fig. 1E**).

Numerous research efforts have delved into enhancing NO production by administering higher L-arginine concentrations to address substrate deficiency in endothelial dysfunction, our study did not reveal any significant difference between healthy and COVID-19.

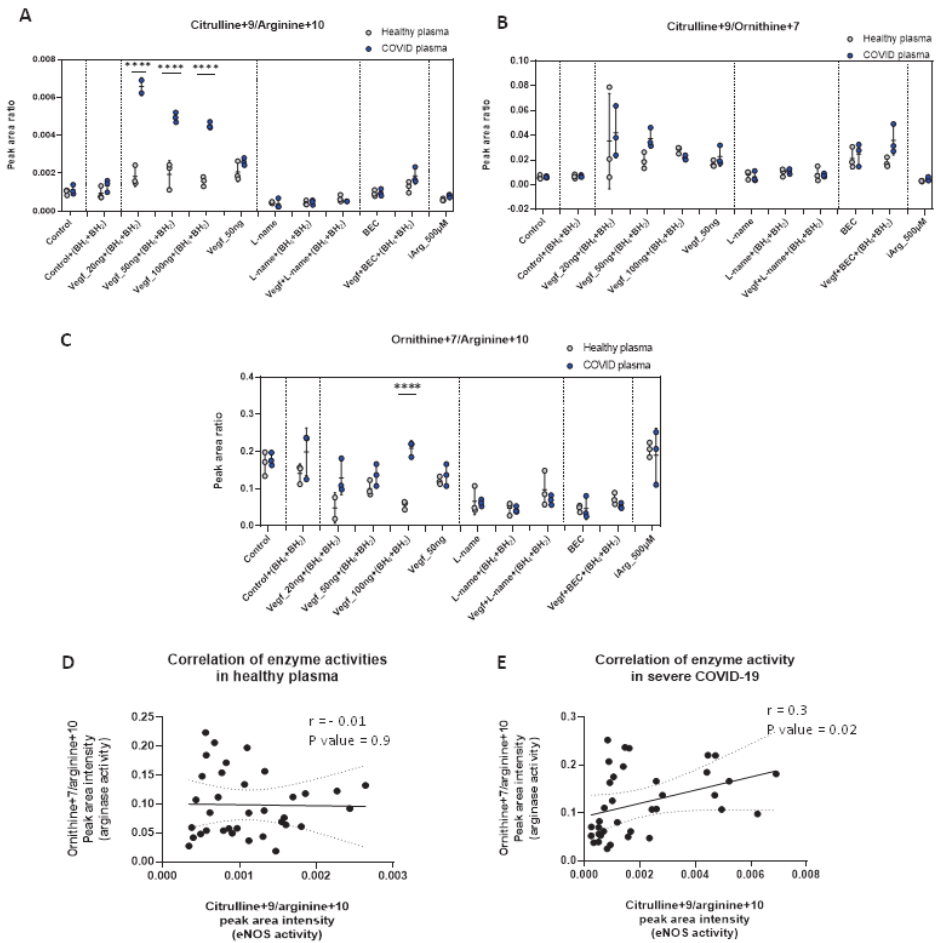


**Figure 1. Measurement of arginine+10, citrulline+9 and ornithine+7 ratios from healthy and PT1 - COVID-19 plasma under stimulatory or inhibitory compound exposure after perfusion through 3D microvessels.** A) The ratio of citrulline+9/arginine+10 B) the ratio of citrulline+9/ornithine+7 and C) the ratio of ornithine+7/arginine+10. Pearson correlation of ornithine+7/arginine+10 and citrulline+9/arginine+10 represents the arginase and eNOS activities D) in healthy plasma ( $r = -0.01$ ,  $p$  value = 0.9) and E) in severe COVID-19 plasma ( $r = 0.3$ ,  $p$  value = 0.02). All error bars represent SD and mean, each dot represents technical replicates,  $n = 3$ . Significance determined by Two-way ANOVA – multiple comparison test of COVID group versus healthy control group. \*,  $P < 0.05$ ; \*\*,  $P < 0.01$ ; \*\*\*,  $P < 0.001$ ; \*\*\*\*,  $P < 0.0001$ .

To understand the impact of COVID on substrate availability, arginine bioavailability was assessed but no significant difference was seen between healthy and COVID-19 conditions (result not shown). Correlation analysis was conducted to assess the relationship between eNOS and arginase enzyme activity. In the healthy cohort (**Fig. 1D**), the correlation analysis revealed an association between eNOS and arginase enzyme activity ( $r = -0.01$ ,  $p$  value = 0.9) and in severe COVID-19 patient, the correlation analysis revealed a significant association between eNOS and arginase enzyme activity ( $r = 0.3$ ,  $P = 0.02$ ), indicating a positive relationship between the two variables. (**Fig. 1E**).

*Measurement of nitric oxide metabolites from mild COVID-19 patient plasma perfused 3D microvessels*

The levels of eNOS-based NO metabolites were measured following the perfusion of plasma samples from mildly infected COVID-19 patient and healthy plasma (control) into the 3D microvessels. Significant differences in NO metabolites assessed using UPLC-MS/MS in a mildly infected COVID-19 patient compared with a healthy control is shown in **Fig. 2 A-C**. The mild condition of COVID-19 was confirmed with the lower viral load, and normal ranges of urea, CRP, albumin, GFR.

The direct measurement of mild COVID-19 plasma shows similar levels of unlabeled citrulline and ornithine in healthy plasma with no statistical difference (**Supplementary Fig. 3A-C**), except arginine levels were higher in COVID-19 plasma.

When analyzing the Citrulline+9/arginine+10 ratio (**Fig. 2A**), no significant changes were observed between healthy and COVID conditions, implying that the utilization of arginine by eNOS for NO production remained consistent in both scenarios. However, in the case of the citrulline+9/ornithine+7 ratio, a significantly lower level was noted in COVID-19 when VEGF+BEC+BH2 was introduced (**Fig. 2B**). This suggests that the relative activity of eNOS to arginase appeared to be notably lower in COVID.

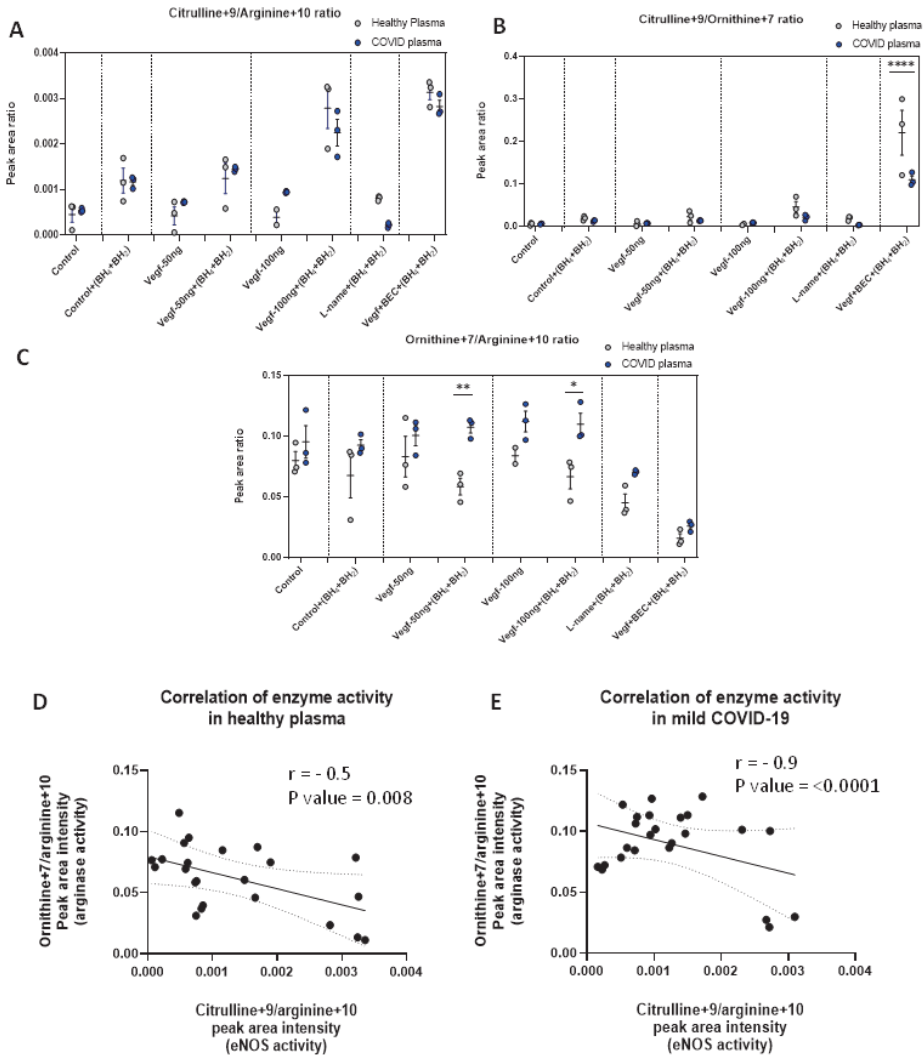


**Figure 2.** Measurement of arginine+10, citrulline+9 and ornithine+7 ratios from healthy and mild COVID-19 plasma under stimulatory or inhibitory compound exposure after perfused into 3D microvessels. A) The ratio of citrulline+9/arginine+10 B) the ratio of citrulline+9/ornithine+7 and C) the ratio of ornithine+7/arginine+10. Pearson correlation of ornithine+7/arginine+10 and citrulline+9/arginine+10 represents the arginase and eNOS activities D) in healthy plasma ( $r = -0.5$ ,  $p \text{ value} = 0.008$ ) and E) in mild COVID-19 plasma ( $r = -0.9$ ,  $p \text{ value} = <0.0001$ ). All error bars represent SD and mean, each dot represents technical replicates,  $n=3$ .

Significance determined by Two-way ANOVA –multiple comparison test of COVID group versus healthy control group. \*, $P < 0.05$ ; \*\*, $P < 0.01$ ; \*\*\*, $P < 0.001$ ; \*\*\*\*, $P < 0.0001$ .

In the COVID-19 context, the introduction of the eNOS stimulator VEGF in the presence of BH4+BH2 resulted in increased levels of the L-ornithine+7/L-arginine+10 ratio (**Fig. 2C**). This indicates that the utilization of arginine by arginase was higher during eNOS stimulation in the presence of the cofactor BH4+BH2, but not in its absence. This suggests that the utilization of arginine+10 to citrulline+9 and ornithine+7 conversion was higher in mild COVID-19. Correlation analysis to assess the relationship between eNOS and arginase activity shows a significant negative correlation in healthy ( $r = -0.5$ ,  $P = 0.008$ ) (**Fig. 2D**) and in COVID-19 ( $r = -0.9$ ,  $P = < 0.0001$ ) (**Fig. 2E**).

### Discussion

Given the ongoing discoveries regarding the enduring effects of COVID-19, it is evident that there is a pressing requirement to create in vitro models for a more profound comprehension of the pathology and consequences of the plasma components. Our 3D microvessels-on-chip model, utilizing collagen as the extracellular matrix and incorporating a microfluidic pump to induce flow, was previously demonstrated to be the optimal experimental setup to study endothelial nitric oxide mechanism [22]. The cell densities and area-to-volume ratios in this model closely mimic physiological conditions [22,29], surpassing those in conventional 2D monolayer cultures. Our study highlights the specific pathways utilizing arginine involved in NO production using our tracer-based method [22]. This study explored how components in COVID-19 plasma might influence eNOS-generated NO and citrulline levels.

In relation to the NO mechanism, our results from severe COVID-19 patient plasma (**Fig. 1A**) support the notion that the BH4+BH2 supplementation with VEGF may improve eNOS coupling in COVID-19, where the NO mechanism may be compromised due to insufficient BH4. Although we did not observe statistically significant changes

with BH<sub>4</sub>+BH<sub>2</sub> supplementation alone when we found a response comparable to that of the healthy condition. The non-significant levels of unlabeled plasma arginine, citrulline and ornithine (**Supplementary Fig. 2A – C**) in clinically confirmed COVID-19 case could reflect that the downstream metabolites (unlabeled ornithine and citrulline) can be produced through other pathways such as glutamine [30,31] or ADMA [32]. However, in mild COVID-19 the significantly higher arginine level indicates the excess of substrate (**Supplementary Fig. 3A – C**).

Through our experimental procedure, it is hypothesized that supplementing BH<sub>4</sub>+BH<sub>2</sub> could elevate BH<sub>4</sub> levels by activating the GTP cyclohydrolase, the first step of BH<sub>4</sub> synthesis along with the presence of shear stress [33]. The significance of citrulline levels in COVID-19 under VEGF+BH<sub>4</sub>+BH<sub>2</sub> treatments was attributed to the previously studied concentration-dependent VEGF increase in NO production [34], leading to higher citrulline+9 levels (**Supplementary Fig. 2D & 3D**) in both severe and mild patients but not such increase was observed in VEGF alone treatment. Other treatment groups showed no significant difference between healthy controls and COVID-19 patients. This could be due to two possible reasons: 1) The lack of a specific stimulus like VEGF, or 2) The inherent presence of BH<sub>4</sub> in the cells or shear stress induced endogenous BH<sub>4</sub> production [33], which might already be sufficient to regulate citrulline levels in these treatment groups in COVID-19 cases.

Under same VEGF+BH<sub>4</sub>+BH<sub>2</sub> treatments, the observed increase in the ornithine+7/arginine+10 ratio (**Fig. 1C & 2C**) in COVID-19 patients receiving VEGF supplementation might be due to the potential feedback mechanism. VEGF stimulates eNOS activity, leading to more L-arginine conversion to citrulline, leaving less L-arginine for arginase, potentially reducing its activity, and causing a slight rise in ornithine levels. Additionally, some studies suggest high ornithine might even feedback and further inhibit arginase, indirectly boosting arginine availability for eNOS [35].

Interestingly, the citrulline+9/ornithine+7 ratio was not indicative in severe COVID-19 (**Fig. 1B**), suggesting similar citrulline and ornithine production across treatments. In mild cases, VEGF+BEC+BH<sub>4</sub>+BH<sub>2</sub> treatment lowered the ratio compared to healthy controls

(**Fig. 2B**). However, the same treatment in mild COVID-19 showed the highest citrulline (**Supplementary Fig. 2D**) levels despite the unclear effect on the ratio.

Increase in ornithine level serves as an indicator of SARS-CoV-2 infection where upregulation of ornithine was reported in earlier studies [36]. In our study, elevated ornithine+7 levels were observed in severe COVID (**Supplementary Fig. 2E**) in higher concentration ( $\leq 500\mu\text{M}$ ) of arginine+10 supplementation, while no significant increase was seen in citrulline+9 (**Supplementary Fig. 2D**). Numerous research efforts have delved into enhancing NO production by administering higher L-arginine concentrations to address substrate deficiency in endothelial dysfunction [37–39], our findings suggest that L-arginine supplementation alone might not be sufficient to significantly increase citrulline levels. While adequate substrate (arginine) was provided, the lack of a sufficient crucial cofactor (BH<sub>4</sub>) seems to be a limiting factor for eNOS activity. This is further supported by the presence of shear stress, a known activator of eNOS, which was already incorporated into the study design.

Maintaining a balanced enzyme activity (eNOS and arginase) and ratio of citrulline to ornithine is essential for optimal nitric oxide (NO) production. Our study suggests that interventions promoting this balance, achieved through BH<sub>4</sub>+BH<sub>2</sub> external supplementation or shear stress-induced production of BH<sub>4</sub>, VEGF treatment in minimal concentrations, and arginase inhibition in both severe and mild COVID-19, show promising therapeutic strategy (**Supplementary Fig. 2D & 3D**). These interventions led to a significant decrease in ornithine levels with BEC/VEGF+BEC+BH<sub>4</sub>+BH<sub>2</sub> treatment. While the effect on the ratio in severe COVID-19 was less pronounced (**Fig. 1B & 2B**), the observed increase in citrulline suggests potential benefits. This approach aims to suppress ornithine production, indirectly promoting citrulline conversion to NO and potentially improving NO production, a crucial molecule for vascular health.

Arginase competes with eNOS for the same substrate, L-arginine. High arginase activity can deplete arginine levels, limiting its availability for eNOS to generate NO. This has led to the exploration of arginase inhibition as a potential therapeutic strategy to address arginine depletion observed in COVID-19 patients [40]. Overall correlation of our treatment strategy revealed a distinct inverse correlation between eNOS and arginase

activity for a mild COVID-19 case when compared to the healthy plasma enzyme activity (**Fig. 2D & 2E**), where eNOS activity increased as arginase activity decreased. Conversely, severe COVID-19 displayed a positive correlation (**Fig. 1E**), potentially reflecting the inflammatory state observed in these patients (**Table 1**).

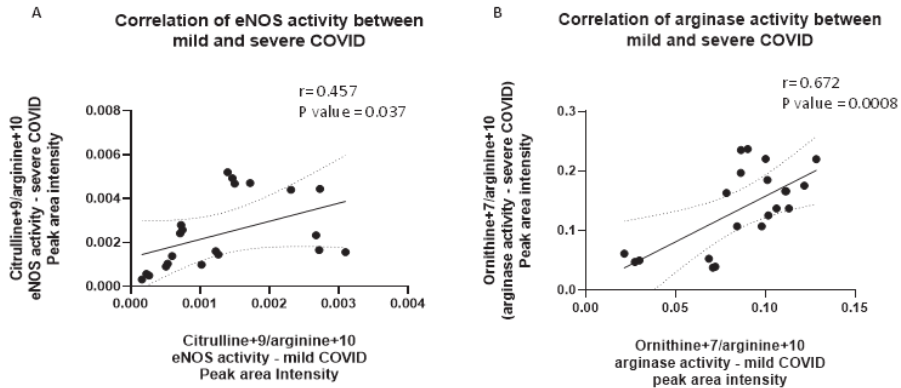


**Figure 3. Measurement of eNOS and arginase enzyme activities in the mild COVID-19 case and the severe COVID-19 case.** Pearson correlation of A) eNOS activity (citulline+9/arginine+10) ( $r = 0.457$ ;  $p \text{ value} = 0.03$ ) and B) arginase activity (ornithine+7/arginine+10) ( $r = 0.672$ ;  $p \text{ value} = 0.0008$ ).

In healthy individuals, arginase and eNOS compete for L-arginine, with eNOS using it for beneficial nitric oxide (NO) production. The positive correlation between these enzymes in severe COVID-19 suggests endothelial dysfunction where the dysregulation of ornithine cycle in COVID-19 was shown in a previous study [41]. eNOS might be upregulated to boost NO production, but arginase activity is not suppressed effectively. This could be due to disrupted arginase regulation or the inflammatory environment of COVID-19 favoring arginase. Ideally, therapies would target both enzymes: upregulating eNOS and suppressing arginase to ensure sufficient L-arginine for NO production. In severe cases, high arginase activity excessively consumes L-arginine, converting it to ornithine. This limits the availability of L-arginine for eNOS to produce NO and

citrulline. Insufficient levels of bioavailable NO are a key factor contributing to endothelial dysfunction [8,42]. Previous studies have reported a strong correlation between hypertension and COVID-19, suggesting an underlying vascular dysfunction [43]. Interestingly, supplementation of BH4 showed to mitigate endothelial dysfunction and oxidative stress in hypercholesterolemic conditions [44] and improved vascular function in heart failure subjects [45]. However, there is limited research on the impact of cofactor supplementation on endothelial dysfunction and NO levels, particularly in the context of COVID-19 recovery.

A correlation analysis was performed to investigate the relationship between eNOS and arginase activity in mild versus severe COVID-19, as shown in **Fig. 3**.

Significantly different and the moderate positive correlation of Arginase and eNOS activities indicates that under various stimuli and inhibitors, both severe and mild COVID-19 cases exhibited similar response patterns, however, the magnitude of the response differed based on the viral load and the disease severity.

### **Conclusion**

The necessity for the best in vitro endothelial model to study COVID-19 arises from the complexity of the disease's effects on the vascular system. In our study we employed a 3D microvessels model, perfusing COVID-19 plasma along with eNOS and arginase enzyme stimulator or inhibitors. This model enabled us to investigate the intricate interactions between endothelial cells and patient plasma components resulting from viral infection, providing insights into the mechanisms underlying COVID-19 pathogenesis. Using a tracer-based UPLC-MS/MS method, perfusing patient plasma samples through the 3D microvessels revealed significant effects on NO metabolites, especially with VEGF and BH4+BH2 supplementation which induced eNOS activity, as seen in higher labeled citrulline levels. Similarly, the interplay between arginase activity and eNOS activity provides insights into the regulatory pathways governing citrulline and ornithine metabolism. This new understanding could serve as a valuable tool for identifying the pathological status associated with vascular diseases. Further investigation into

therapeutic strategies utilizing eNOS stimulation alongside arginase inhibition is warranted based on these results. Finally, our study stands out as we observe a distinct response of NO metabolites based on the clinical data and disease severity of each patient. This model is highly recommended for investigating the impact of plasma components on endothelial cells, especially given our understanding of the detailed eNOS mechanism. Furthermore, such models facilitate the evaluation of potential therapeutics and interventions targeting endothelial dysfunction, inflammation, thrombosis, and other vascular complications associated with COVID-19.

### **Limitations of the study**

This preliminary study underscores the need for additional patient samples to establish a broader conclusion. Moreover, insights from patients' pathological history, medication practices, and clinical reports pertaining to endothelial dysfunction would be valuable. Furthermore, measuring downstream metabolites of BH<sub>4</sub>, such as BH<sub>2</sub> and neopterin, could provide additional validation to our study and also provide insights into the importance of BH<sub>4</sub> in the eNOS mechanism and potentially serve as a more effective therapeutic target.

### **Acknowledgements**

Parts of these studies were supported by the Dutch Heart Foundation (CVON RECONNECT) and ZonMW (MKMD: 114022501) grants to T.H and A.J.V.Z. Part was supported by METABODELTA (Medical Delta program). This project has received funding from the European Union's Horizon 2020 research and innovation Programme LogicLab under the Marie Skłodowska-Curie grant agreement No 813920, and RECONNEXT funded by the Dutch Heart Foundation No 2020B008.

We would like to acknowledge the contributions of Sam Heijjer, Sabine Bos, and Mengle Zhu to the initial analysis of biopterin compounds. Additionally, we would like

to express our sincere gratitude to Faisa Guled for her help in developing the mass spectrometry method for measuring these compounds.

### **Author Contributions**

Kanchana Pandian, Conceptualization, Investigation, Methodology, Writing - original draft;

Rudmer Postma, Writing – review and editing;

Anton Jan van Zonneveld, Amy Harms, and Thomas Hankemeier, Conceptualization, Resources, Supervision, Funding acquisition, Writing – review and editing.

### **Declaration of interest**

T. Hankemeier is a shareholder in Mimetas B.V. All other authors declare no competing interests.

### **Data availability statement**

The data that support the findings of this study are available in the Materials and Methods, Results, and Supplementary Material of this article. Additional data will be provided upon request.

### **References**

[1] Pathak, B.D. et al. (2023). Oxygen Requirement and Associated Risk Factors in Post-COVID-19 Patients Admitted to a Tertiary Care Center: A Cross-Sectional Study. *The Canadian Journal of Infectious Diseases & Medical Microbiology = Journal Canadien des Maladies Infectieuses et de la Microbiologie Médicale*. <https://doi.org/10.1155/2023/3140708>.

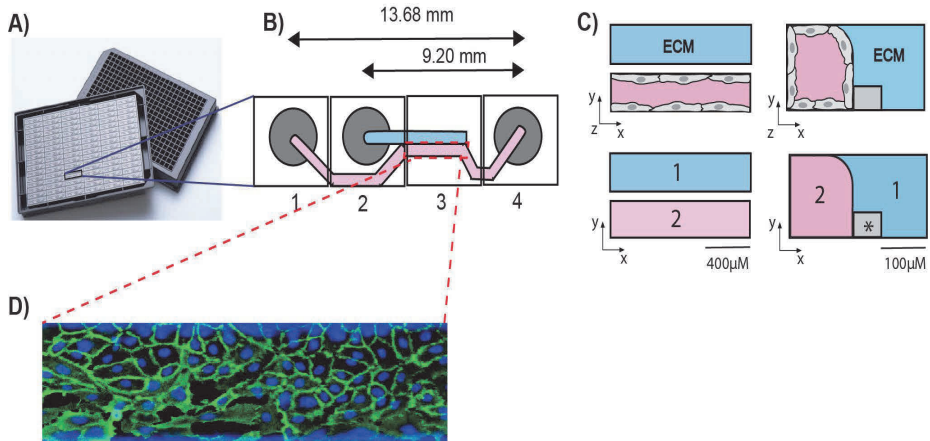
[2] Varga, Z. et al. (2020). Endothelial cell infection and endotheliitis in COVID-19. *The Lancet*. [https://doi.org/10.1016/S0140-6736\(20\)30937-5](https://doi.org/10.1016/S0140-6736(20)30937-5).

- [3] Ackermann, M. et al. (2020). Pulmonary Vascular Endothelialitis, Thrombosis, and Angiogenesis in Covid-19. *New England Journal of Medicine*. <https://doi.org/10.1056/NEJMoa2015432>.
- [4] Giordo, R. et al. (2021). SARS-CoV-2 and endothelial cell interaction in COVID-19: molecular perspectives. *Vascular Biology*. <https://doi.org/10.1530/VB-20-0017>.
- [5] Nagashima, S. et al. (2020). Endothelial Dysfunction and Thrombosis in Patients With COVID-19—Brief Report. *Arteriosclerosis, Thrombosis, and Vascular Biology*. <https://doi.org/10.1161/ATVBAHA.120.314860>.
- [6] Pelle, M.C. et al. (2022). Endothelial Dysfunction in COVID-19: Potential Mechanisms and Possible Therapeutic Options. *Life*. <https://doi.org/10.3390/life12101605>.
- [7] Teuwen, L.-A. et al. (2020). COVID-19: the vasculature unleashed. *Nature Reviews Immunology*. <https://doi.org/10.1038/s41577-020-0343-0>.
- [8] Green, S.J. (2020). Covid-19 accelerates endothelial dysfunction and nitric oxide deficiency. *Microbes and Infection*. <https://doi.org/10.1016/j.micinf.2020.05.006>.
- [9] Herrera, M.D. et al. (2010). Endothelial dysfunction and aging: An update. *Ageing Research Reviews*. <https://doi.org/10.1016/j.arr.2009.07.002>.
- [10] Guan, S.P. et al. (2020). Does eNOS derived nitric oxide protect the young from severe COVID-19 complications? *Ageing Research Reviews*. <https://doi.org/10.1016/j.arr.2020.101201>.
- [11] Glynn, J.R. and Moss, P.A.H. (2020). Systematic analysis of infectious disease outcomes by age shows lowest severity in school-age children. *Scientific Data*. <https://doi.org/10.1038/s41597-020-00668-y>.
- [12] Akaberi, D. et al. (2020). Mitigation of the replication of SARS-CoV-2 by nitric oxide in vitro. *Redox Biology*. <https://doi.org/10.1016/j.redox.2020.101734>.
- [13] Alvarez, R.A. et al. (2020). Home Nitric Oxide Therapy for COVID-19. *American Journal of Respiratory and Critical Care Medicine*. <https://doi.org/10.1164/rccm.202005-1906ED>.
- [14] Nishimura, M. et al. (1995). Nitrogen Dioxide Production during Mechanical Ventilation with Nitric Oxide in Adults : Effects of Ventilator Internal Volume, Air Versus Nitrogen Dilution, Minute Ventilation, and Inspired Oxygen Fraction. *Anesthesiology*. <https://doi.org/10.1097/00000542-199505000-00020>.
- [15] Förstermann, U. and Sessa, W.C. (2012). Nitric oxide synthases: regulation and function. *European Heart Journal*. <https://doi.org/10.1093/eurheartj/ehr304>.
- [16] Martínez-Gómez, L.E. et al. (2022). Metabolic Reprogramming in SARS-CoV-2 Infection Impacts the Outcome of COVID-19 Patients. *Frontiers in Immunology*.
- [17] Maier, W. et al. (2000). Tetrahydrobiopterin Improves Endothelial Function in Patients with Coronary Artery Disease. *Journal of Cardiovascular Pharmacology*.
- [18] Swathi Krishna, S. et al. (2022). Dietary foods containing nitric oxide donors can be early curators of SARS-CoV-2 infection: A possible role in the immune system. *Journal of Food Biochemistry*. <https://doi.org/10.1111/jfbc.13884>.

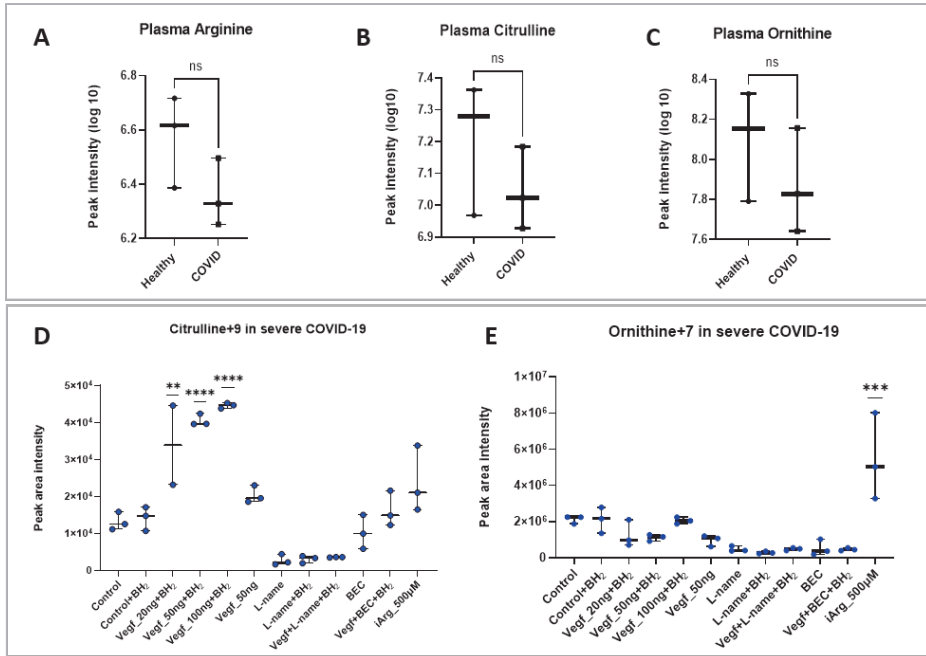
- [19] Fang, W. et al. (2021). The role of NO in COVID-19 and potential therapeutic strategies. *Free Radical Biology & Medicine*.  
<https://doi.org/10.1016/j.freeradbiomed.2020.12.008>.
- [20] Junaid, A. et al. (2020). Ebola Hemorrhagic Shock Syndrome-on-a-Chip. *iScience*.  
<https://doi.org/10.1016/j.isci.2019.100765>.
- [21] Junaid, A. et al. (2021). A Microfluidics-Based Screening Tool to Assess the Impact of Blood Plasma Factors on Microvascular Integrity. *Advanced Biology*.  
<https://doi.org/10.1002/adbi.202100954>.
- [22] Pandian, K. et al. (2023). Tracer-based metabolomics for profiling nitric oxide metabolites in a 3D microvessel-on-a-chip model. <https://doi.org/10.1101/2023.12.03.569402>.
- [23] Abdullah, A.J. et al. (2023). Assessing serum C-reactive protein as a predictor of COVID-19 outcomes: a retrospective cross-sectional study. *Annals of Medicine and Surgery*.  
<https://doi.org/10.1097/MS9.0000000000000761>.
- [24] Hosten, A.O. (1990). BUN and Creatinine, in *Clinical Methods: The History, Physical, and Laboratory Examinations*, 3rd ed., Butterworths, Boston.
- [25] Moman, R.N. et al. (2024). Physiology, Albumin, in *StatPearls*, StatPearls Publishing, Treasure Island (FL).
- [26] Gounden, V. et al. (2024). Renal Function Tests, in *StatPearls*, StatPearls Publishing, Treasure Island (FL).
- [27] Delongui, F. et al. (2013). Serum Levels of High Sensitive C Reactive Protein in Healthy Adults From Southern Brazil. *Journal of Clinical Laboratory Analysis*.  
<https://doi.org/10.1002/jcla.21585>.
- [28] Noga, M.J. et al. (2012). Metabolomics of cerebrospinal fluid reveals changes in the central nervous system metabolism in a rat model of multiple sclerosis. *Metabolomics: Official Journal of the Metabolomic Society*. <https://doi.org/10.1007/s11306-011-0306-3>.
- [29] van Duinen, V. et al. (2017). 96 perfusable blood vessels to study vascular permeability in vitro. *Scientific Reports*. <https://doi.org/10.1038/s41598-017-14716-y>.
- [30] Windmueller, H.G. and Spaeth, A.E. (1981). Source and fate of circulating citrulline. *American Journal of Physiology-Endocrinology and Metabolism*.  
<https://doi.org/10.1152/ajpendo.1981.241.6.E473>.
- [31] Windmueller, H.G. and Spaeth, A.E. (1974). Uptake and Metabolism of Plasma Glutamine by the Small Intestine. *Journal of Biological Chemistry*.  
[https://doi.org/10.1016/S0021-9258\(19\)42329-6](https://doi.org/10.1016/S0021-9258(19)42329-6).
- [32] Pai, J.K. (2008). Asymmetric dimethylarginine as a marker of metabolic dysfunction and cardiovascular disease. *Current Cardiovascular Risk Reports*. <https://doi.org/10.1007/s12170-008-0028-x>.
- [33] Widder, J.D. et al. (2007). Regulation of tetrahydrobiopterin biosynthesis by shear stress. *Circulation Research*. <https://doi.org/10.1161/CIRCRESAHA.107.153809>.

- [34] Papapetropoulos, A. et al. (1997). Nitric oxide production contributes to the angiogenic properties of vascular endothelial growth factor in human endothelial cells. *Journal of Clinical Investigation*.
- [35] Durante, W. et al. (2007). Arginase: a critical regulator of nitric oxide synthesis and vascular function. *Clinical and Experimental Pharmacology & Physiology*.  
<https://doi.org/10.1111/j.1440-1681.2007.04638.x>.
- [36] Rees, C.A. et al. (2021). Altered amino acid profile in patients with SARS-CoV-2 infection. *Proceedings of the National Academy of Sciences of the United States of America*.  
<https://doi.org/10.1073/pnas.2101708118>.
- [37] Ströhle, A. et al. (2016). [L-Arginine and vascular health]. *Medizinische Monatsschrift Fur Pharmazeuten*.
- [38] Adebayo, A. et al. (2021). L-Arginine and COVID-19: An Update. *Nutrients*.  
<https://doi.org/10.3390/nu13113951>.
- [39] Reizine, F. et al. (2021). SARS-CoV-2-Induced ARDS Associates with MDSC Expansion, Lymphocyte Dysfunction, and Arginine Shortage. *Journal of Clinical Immunology*.  
<https://doi.org/10.1007/s10875-020-00920-5>.
- [40] Grimes, J.M. et al. (2021). Arginine depletion as a therapeutic approach for patients with COVID-19. *International journal of infectious diseases: IJID: official publication of the International Society for Infectious Diseases*. <https://doi.org/10.1016/j.ijid.2020.10.100>.
- [41] Li, T. et al. (2021). Longitudinal Metabolomics Reveals Ornithine Cycle Dysregulation Correlates With Inflammation and Coagulation in COVID-19 Severe Patients. *Frontiers in Microbiology*. <https://doi.org/10.3389/fmicb.2021.723818>.
- [42] Cyr, A.R. et al. (2020). Nitric Oxide and Endothelial Dysfunction. *Critical care clinics*. <https://doi.org/10.1016/j.ccc.2019.12.009>.
- [43] Yoshihara, F. (2024). Association between blood pressure and COVID-19 severity. *Hypertension Research*. <https://doi.org/10.1038/s41440-023-01557-8>.
- [44] Cosentino, F. et al. (2008). Chronic treatment with tetrahydrobiopterin reverses endothelial dysfunction and oxidative stress in hypercholesterolaemia. *Heart*.  
<https://doi.org/10.1136/hrt.2007.122184>.
- [45] Bunsawat, K. et al. (2022). The Impact of Short-Term Tetrahydrobiopterin (BH4) Supplementation on Peripheral Vascular Function in Heart Failure with Preserved Ejection Fraction (HFpEF). *The FASEB Journal*. <https://doi.org/10.1096/fasebj.2022.36.S1.R3751>.

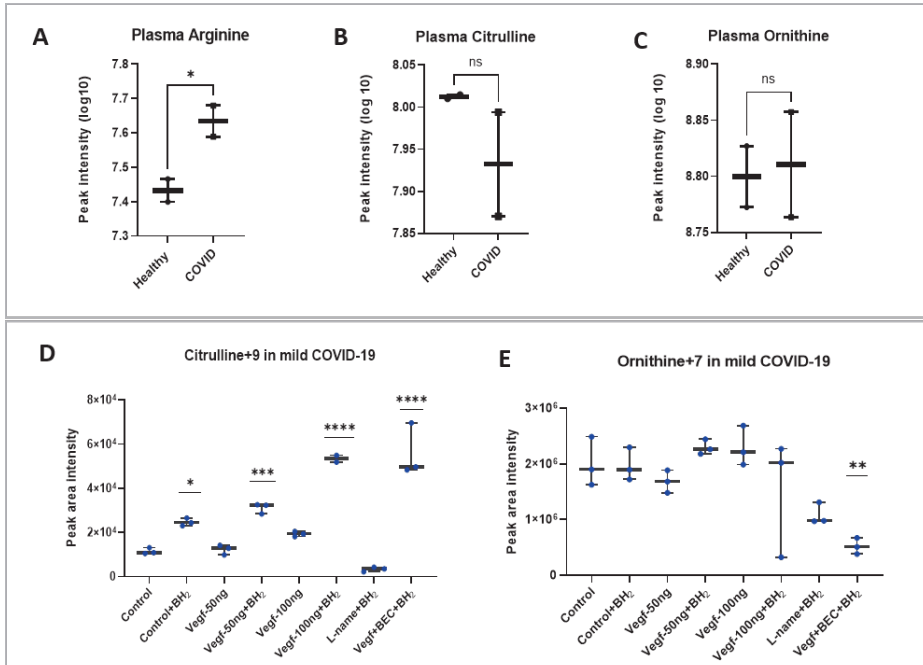
Supplementary Information



**Supplementary Figure 1.** Illustration of (A) re-routed OrganoPlate and its (B) Single chip design was explained below. Every microfluidic chip structure is positioned underneath 4 adjacent wells and it consists of two channels: 1) an ‘perfusion’ channel (pink color) and 2) a ‘gel’ channel (ECM) (blue color). Every first well (1) and fourth well (4) is positioned on top of the inlet and outlet of the perfusion channel, while every second well (2) are for the gel channel. And every third well (3) is used for imaging and observation of the experiment. (C) Perfusion and gel channel was shown vertical and horizontal view and its separated by a phase guide (\*). (D) Immunostaining of HCAECs in a chip. After 48 hours of cell seeding, a confluent vessel of HCAECs were immunostained with V-Cadherin and DAPI. After treatment with plasma and other compounds, the perfusate was collected from the outlet of each micro vessel for subsequent metabolic analysis.



**Supplementary Figure 2.** Measurement of A) unlabeled arginine, B) unlabeled citrulline, and C) unlabeled ornithine from healthy and severe COVID-PT1 plasma before perfusion through the 3D microvessels. D) Measurement of citrulline+9 and E) ornithine+7 from healthy and severe COVID-19 plasma under stimulatory or inhibitory compound exposure after perfusion through 3D microvessels. All error bars represent SD and mean, each dot represents a technical replicate, n=3-4. Significance was determined by student t-test and two-way ANOVA –multiple comparison test of healthy control versus COVID group. \*,P<0.05; \*\*,P<0.01; \*\*\*,P <0.001; \*\*\*\*,P<0.0001, ns = non-significant.



**Supplementary Figure 3.** Measurement of A) unlabeled arginine, B) unlabeled citrulline, and C) unlabeled ornithine from healthy and mild COVID-19 (PT2) plasma before perfusion through the 3D microvessels. D) Measurement of citrulline+9 and E) ornithine+7 from healthy and mild - COVID-19 plasma under stimulatory or inhibitory compound exposure after perfusion through 3D microvessels. All error bars represent SD and mean, each dot represents a technical replicate, n=3-4. Significance was determined by student t-test and two-way ANOVA –multiple comparison test of healthy control versus COVID group. \*,P<0.05; \*\*,P<0.01; \*\*\*,P <0.001; \*\*\*\*,P<0.0001, ns = non-significant.

### Targeted LC-MS/MS method for BH4 and BH2

Targeted LC-MS/MS analysis was performed for BH4 and BH2 measurement using an ultra-performance liquid chromatography coupled to tandem mass spectrometry (UPLC-MS/MS) system Class I (Acquity, Waters Chromatography Europe BV, Etten-Leur, The Netherlands) system with an SeQuant® ZIC®-cHILIC column (2.1 mm × 100 mm, 3.0

$\mu$ m- Merck, Darmstadt, Germany) coupled to a Sciex QTRAP® 6500 mass spectrometer. Detailed descriptions of the measurement methods can be found in the supplementary material.

The LCMS method was adapted from the previous work [28] with some modifications. Briefly, mobile phase A consisted of 90% acetonitrile and 10% 5 mM ammonium formate. Mobile phase B consisted of 10% acetonitrile, 90% 5 mM ammonium formate. The aqueous 5 mM ammonium formate was adjusted to pH 7.4 using formic acid or ammonium hydroxide. The ZIC-c column is composed of silica-based particles (1:1 charge-balanced phosphorylcholine functional group) which lose stability in pH above 8. Therefore, the ZIC-c was operated only at acidic and neutral conditions.

The flow rate was 0.50 mL/min with the following mobile phase gradient: 0.0–1.0 min (0% B), 1.0–2.0 min (0-15% B), 2.0–5.0 min (15-21% B), 5.0–6.0 min (21-40% B), 6.0–7.0 min (40% B), 7.0–7.5 min (40-0% B), 7.5–12.5 min (0% B).

BH4 and BH2 standards were obtained from Sigma-Aldrich (The Netherlands) and the details were shown in **Suppl. Table 2**. Both the standards were accurately weighed and prepared in an appropriate solution to obtain the individual stock solution at a concentration of 100 $\mu$ M to prepare calibration solutions of concentrations 2 $\mu$ M, 5 $\mu$ M, 10 $\mu$ M, 25 $\mu$ M, 50 $\mu$ M and 100 $\mu$ M.

Mass spectrometry experiments were carried out on a Sciex QTRAP® 6500 mass spectrometer. Electrospray ionization (ESI) was operating in positive ion mode. The ESI source parameters were as follows (positive ion mode): spray voltage  $\pm 4.5$  kV, capillary temperature 250 °C, sheath gas 40, auxiliary gas 45, curtain gas 30.

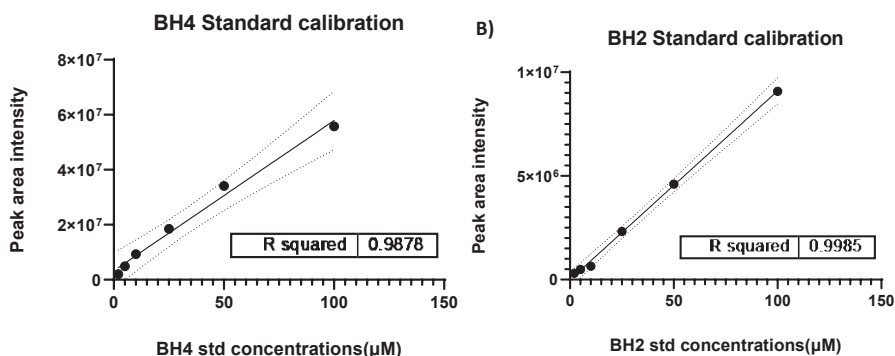
### ***Measurement of BH4 and BH2***

Mass spectrometry analysis revealed a significantly higher abundance of fragment ions at  $m/z$  241.11/166 for BH4 and 239.10/164  $m/z$  for BH2 compared to other fragmentation products. The compound list with observed mass adducts and  $m/z$  ratios is shown in **Supplementary Table 2**. Raw LC-MS/MS data was processed with AB Sciex PeakView™ 2.0 and MultiQuant™ 3.0.1 software for targeted metabolite peak

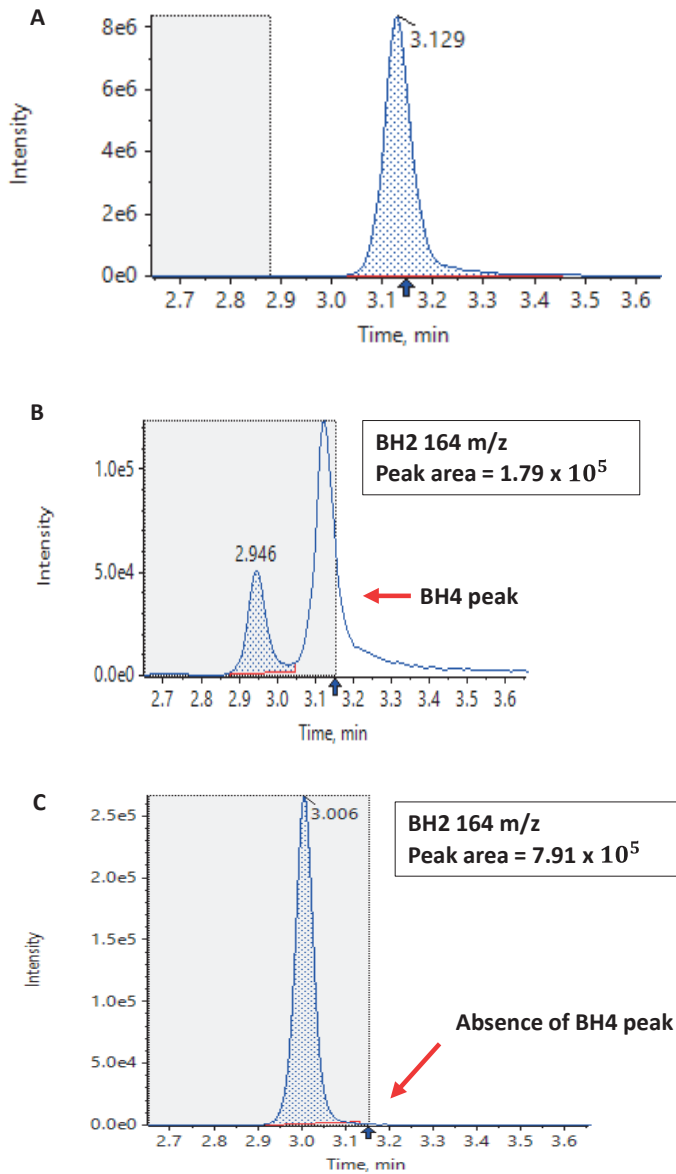
identification and integration. We included calibration curves for each standard in **Supplementary Fig. 4**.

We assessed BH4's susceptibility to oxidation at room temperature by comparing its behavior in the presence and absence of 1 mM dithiothreitol (DTT, Sigma Aldrich, Netherlands), a common antioxidant. In both scenarios, BH4 displayed limited stability, readily converting to BH2 (**Supplementary Fig. 5A & 5B**). Even BH4 standards stored at  $-80^{\circ}\text{C}$  exhibited similar instability when measured the following day, with complete conversion to BH2 observed (**Supplementary Fig. 5C**).

Due to the inherent instability of BH4 during direct measurement, the BH4 standard likely oxidized to BH2. Consequently, we report BH4+BH2 in the results to reflect the actual form detected by mass spectrometry. Independent verification of these metabolites in extracts is crucial for definitive identification.



**Supplementary Figure 4.** Calibration curves of BH4 and BH2 with concentrations - 2  $\mu\text{M}$ , 5  $\mu\text{M}$ , 10  $\mu\text{M}$ , 25  $\mu\text{M}$ , 50  $\mu\text{M}$ , and 100  $\mu\text{M}$ . Note: Higher calibration concentrations was used due to the high susceptibility of the analyte to oxidation.



**Supplementary Figure 5. Measurement of BH4 standard (50 $\mu$ M) by direct injection and the stability check.** A) Peak of BH4 standard (241.11/166 m/z) on day 1, B) Oxidation of BH4 to BH2(239.10/164 m/z) an hour after standard solution preparation, and C) Peak intensity comparison showing complete oxidation of BH4 to BH2 after 12 hours at room temperature. Note: BH4 standard was prepared using 90% acetonitrile and 10% 5mM ammonium formate adjusted to

pH 7.4. BH2 standard was prepared using 10% DMSO in 90% acetonitrile and 10% 5mM ammonium formate (pH 7.4).

**Supplementary Table 1.** MRM method and the compound list with target m/z for precursor and product ions for tracer metabolites measurement.

Metabolites name	Mass (Q1)	Mass (Q3)
L-arginine	345.170	171.00
L-arginine [M+10]	355.170	171.00
L-citrulline	346.150	171.00
L-citrulline [M+9]	355.150	171.00
L-ornithine	237.100	171.00
L-ornithine [M+7]	240.600	171.00

**Supplementary Table 2.** Details of BH4 and BH2 standards used in the study.

Compound	CHEBI ID	Supplier	Class	Formula	Mass adducts	ESI m/z	Stock concentration (mM)	Stock solvent
BH4	15372	Sigma-Aldrich	Pteridines	C <sub>9</sub> H <sub>15</sub> N <sub>5</sub> O <sub>3</sub> · 2HCl	[M+H] <sup>+</sup>	241.1175 166, 107,149	1	90% acetonitrile and 10% 5 mM ammonium formate
BH2	64277	Sigma-Aldrich	Pteridines	C <sub>9</sub> H <sub>13</sub> N <sub>5</sub> O <sub>3</sub>	[M+H] <sup>+</sup>	239.1018 164, 168, 196	1	10% DMSO in 90% acetonitrile and 10% 5 mM ammonium formate